Dynamics of a driven lower polariton mode in resonantly excited planar GaAs microcavities

A. A. Demenev,[1] A. A. Shchekin,[1] A. V. Larionov,[1] S. S. Gavrilov,[1,2] and V. D. Kulakovskii[1]
[1]*Institute of Solid State Physics, RAS, Chernogolovka 142432, Russia*
[2]*A. M. Prokhorov General Physics Institute, RAS, Moscow 119991, Russia*
(Received 10 November 2008; revised manuscript received 12 February 2009; published 9 April 2009)

Instabilities in a driven lower polariton (LP) mode in planar GaAs microcavities are investigated under the resonant optical pumping near the magic angle, with the use of a time-resolved technique. A qualitatively different hysteresis behavior has been observed for the intracavity field $\mathcal{E}_{QW}$ and for the resonance energy of the driven LP mode. Self-instability of the driven nonlinear LP oscillator, which develops with increasing pumping, results in a sharp increase in both $\mathcal{E}_{QW}$ and the LP energy. The steplike increase in $\mathcal{E}_{QW}$ transfers the LP system in a region of its strong parametric instability with respect to the intermode scattering. The instability mainly results in a redistribution of LPs in the momentum space, which causes a strong decrease in $\mathcal{E}_{QW}$ for the driven mode but weakly affects the resonance energy. The results are qualitatively explained within a coherent many-mode approximation based on the Gross-Pitaevskii equations.

DOI: 10.1103/PhysRevB.79.165308 PACS number(s): 71.36.+c, 42.65.Pc, 42.55.Sa

I. INTRODUCTION

Quasi-two-dimensional (2D) excitonic polaritons in semiconductor microcavities (MCs) have attracted strong interest since a pioneering work by Weisbuch *et al.*,[1] where the strong coupling of 2D exciton with a cavity photon was demonstrated. A lot of interesting effects can be expected, which are due to the bosonic nature of polaritons, as well as due to their extremely small effective mass and the presence of an inflection point in the lower polariton (LP) dispersion branch.[2–21] One of the most striking phenomena is the giant rate of stimulated polariton-polariton scattering that starts, in case of optical excitation at wave vector $\mathbf{k}_p$ close to the inflection point, $\mathbf{k}=\mathbf{k}_{\mathrm{infl}}$, at an unusually low excitation density.[11–21] The scattering does not follow a key prediction of the conventional four-wave mixing theory. Instead of a shift along the dispersion curve in response to a shift of $\mathbf{k}_p$ and/or the excitation energy E_p, the "signal" and "idler" appear invariably at $\mathbf{k}\sim 0$ and $\sim 2\mathbf{k}_p$, respectively, being blueshifted from the LP dispersion curve.[20,21]

Suggested models for stimulated polariton-polariton scattering are mostly based on the optical parametric oscillator (OPO) model that considers all the k states of polaritons as classical oscillators and takes into account the pairwise (polariton-polariton) interaction.[22–32] Respective equations are similar to the Gross-Pitaevskii equations used in theories of the weakly imperfect Bose gas.

Practically, the OPO-based model is often reduced to consideration of three macro-occupied modes (i.e., pump, signal, and idler modes; see Refs. 22–26 and 29). In general, this approximation provides a qualitative explanation of the threshold behavior of stimulated scattering, but cannot explain the certain direction of the scattering signal. At the same time, valuable efforts were aimed at investigation of stationary (time-independent) solutions of the reduced three-mode system.[22–26] However, formation of a stationary state (that, presumably, may appear when all the "fast" processes related to the development of instability are already finished) is only one of possible opportunities for the system dynamics. Under the strongly nonequilibrium conditions corresponding to the case of coherent resonant excitation, the system may eventually pass to a nonstationary state such as a limit cycle or even a more complicated attractor of the phase-space trajectory.

Beyond the scope of above-mentioned approximations, behavior of a resonantly driven LP system was considered in the framework of many-mode OPO-based model with all the pairwise interactions included.[30–34] Stability analysis of the driven LP mode and numerical simulations of evolution of the many-mode system were performed within a unified approach. The unusual behavior of the stimulated scattering under the excitation at "magic angle" ($\mathbf{k}_p\sim\mathbf{k}_{\mathrm{infl}}$) was shown to be coming from an interplay between two distinct instabilities arising in the driven system. These are, first, a single-mode bistability with respect to the external pump[35] and, second, a parametric instability with respect to a decay into multiple scattered LP states. The system evolution path as well as its final state was found to be crucially dependent on the process of instability development (see Ref. 36).

Optical bistability in a triply resonant OPO system (i.e., with the cavity being simultaneously resonant to the pump, signal, and idler modes) was observed several years ago.[37] Recently, the bistability for an isolated LP mode driven externally was reported for excitation at $\mathbf{k}_p=0$.[24] It originates from Kerr-type (cubic) nonlinearity caused by the self-action of a driven mode. Later, the same authors observed the hysteresis effect in the MC emission normal to the cavity plane under cw excitation at $\mathbf{k}_p=\mathbf{k}_{\mathrm{infl}}$.[2] In the latter case the hysteresis results from the intermode interaction. The obtained results were qualitatively explained within a three-mode OPO model, which allowed the authors to conclude that there is the fundamental analogy between the system of LPs in a planar MC and a three-mode OPO system.

It is of importance, however, that the cw techniques are unable to distinguish intermediate states for different evolution paths for the excited system. Because of that, they are not sufficient for investigation of processes that involve concurrent development of several instabilities. As a result, cw techniques are unable to clarify the dynamical way of appearance of macro-occupied signal at $\mathbf{k}\sim 0$.

To trace the development of instabilities, the time-resolved techniques should be employed. Recently such a technique was used to study the kinetics of stimulated polariton scattering excited by nanosecond-long pulses.[38] Compared to the LP lifetime of a few picoseconds, the excitation conditions may be considered as a quasistationary pump.[39] The studies showed the three-mode OPO model failing to describe the formation of the scattering signal at $\mathbf{k}\approx 0$. On reaching the threshold, the scattering initially goes into a wide range of k vectors, whereas the signal at $\mathbf{k}\approx 0$ appears as a result of self-organization in the excited polariton system.

In the present study, we employed the time-resolved technique to investigate the instabilities in the driven LP mode in detail. Time evolution of the magnitude of the signal passing through the cavity and the spectral position of the driven LP mode are studied. Critical transformations of the driven mode due to its instabilities are traced, both the stable and the transient states of the driven LP oscillator are detected, and the effect of the interplay between the self-instability and the intermode decay instability of the driven mode on the evolution of pumped LP system is revealed.

The paper is organized as follows. In Sec. II, the sample structure and experimental setup are described. Section III presents experimental studies of the time evolution of intensity (Sec. III A) and spectral position (Sec. III B) of the intracavity optical field in the driven LP mode. Finally, comparison of the experimental results to the available theoretical OPO models is given in Sec. III C.

II. EXPERIMENT

MC structure consisted of two Bragg reflectors with 17 and 20 repeats of $\lambda/4$ $Al_{0.13}Ga_{0.87}As/AlAs$ layers in the top and rear mirrors, respectively, and a $3\lambda/2$ active layer between them. The active layer contained six 10-nm-thick $In_{0.06}Ga_{0.94}As/GaAs$ quantum wells (QWs). Rabi splitting of the coupled exciton-cavity modes was $\Omega\approx 6$ meV. The sample was placed into an optical cryostat at the temperature of 7 K. Resonant excitation was produced by a pulsed Ti-sapphire laser (with picosecond-long pulses) at a repetition rate of 5 kHz and delivered to the cryostat using a long multimode optical fiber. After the fiber, the pulses had duration of ~ 1 ns and the spectral full width at half maximum (FWHM) of about 0.9 meV. The average excitation power was varied from 3 to 20 μW.

The angle between the pump laser beam and the normal to the sample was 14° ($k_p\approx 1.8\times 10^4$ cm^{-1}). The k-space distribution for the excited LPs was measured by selecting the detection angle θ. The latter is connected to k as $k=(\omega/c)\sin\theta$, where ω is the light frequency. Both the kinetics of the transmission signal and that of MC luminescence were measured from the opposite to the pump side of the cavity. The signal was detected by a streak camera with spectral resolution of 0.2 meV and temporal resolution of 70 ps. Excitation beam was always focused onto the same spot, which was 100 μm in diameter. Detuning between the exciton $E_X(k=0)$ and photon $E_C(k=0)$ modes in the excitation spot was found to be $E_C-E_X\approx -2$ meV.

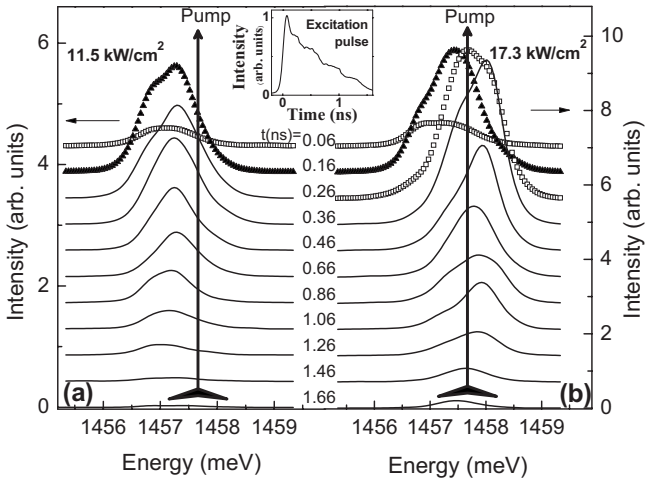

FIG. 1. Transmission spectra recorded at $\mathbf{k}=\mathbf{k}_p$ with time separation delay of 100–200 ps from 0.06 to 1.66 ns at the excitation densities (a) $P=11.3$ and (b) 17.3 kW/cm^2. The value P corresponds to the peak values of $I_{\text{ext}}(t)$. The spectral position of the excitation pulse is shown by gray vertical arrows labeled as "Pump." The pump pulse profile $I_{\text{ext}}(t)$ is shown in the inset.

III. EXPERIMENTAL RESULTS AND DISCUSSION

A. Instabilities and hysteresis behavior for the intracavity optical field in the driven LP mode

Data on the driven LP mode instabilities were obtained from MC transmission measurements. The active region in the cavity is separated from the detector by a Bragg mirror that does not introduce any nonlinearity and/or spectral selectivity. Because of that, the intensity of the pump pulse transmitted through the MC, $I_{\text{tr}}(\omega,t)$, is proportional to the squared magnitude of the intracavity electric field, $|\mathcal{E}_{\text{QW},\mathbf{k}_p}(\omega,t)|^2$, and therefore provides direct information of its spectral and time dependences.[40] The time dependence of a spectrally integrated intensity, $\int I_{\text{tr}}(\omega,t)d\omega=I_{\text{tr}}(t)$, is proportional to the squared magnitude of electric field at the excitation k-vector $|\mathcal{E}_{\text{QW}}(\mathbf{k}_p,t)|^2$, whereas the time dependence of the first momentum $\int\hbar\omega I_{\text{tr}}(\omega,t)d\omega/\int I_{\text{tr}}(\omega,t)d\omega$ gives one the information on the change in an average energy of excited LP mode, $\tilde{E}_{\text{LP}}(t)$.

The pump pulse profile $I_{\text{ext}}(t)$ is shown in the inset of Fig. 1. Note that it is proportional to the intensity of the external electric field outside the MC, $|\mathcal{E}_{\text{ext}}(\mathbf{k}_p,t)|^2$. The pump intensity builds up during the first 100 ps and then decreases slowly (by about three times by $t=1$ ns). The pulses of a circular (σ^+) polarization and the FWHM of 0.9 meV excite the MC about 0.5 meV above the LP dispersion branch at $\mathbf{k}_p=(k_{px},k_{py})=(1.8,0)$ μm^{-1}.

Figures 1(a) and 1(b) show the transmission spectra recorded at $k=k_p$ with the time interval of 100–200 ps at the excitation densities $P=11.3$ and 17.3 kW/cm^2, respectively. The value P identifies the maximum values of $I_{\text{ext}}(t)$, $P=\max_t I_{\text{ext}}(t)$. Figure 1 demonstrates that both the spectral position and the FWHM of the transmission signal recorded at the low excitation density change very weakly during the pulse duration. Meanwhile, the spectra recorded at the high pumping density demonstrate a well-pronounced broadening

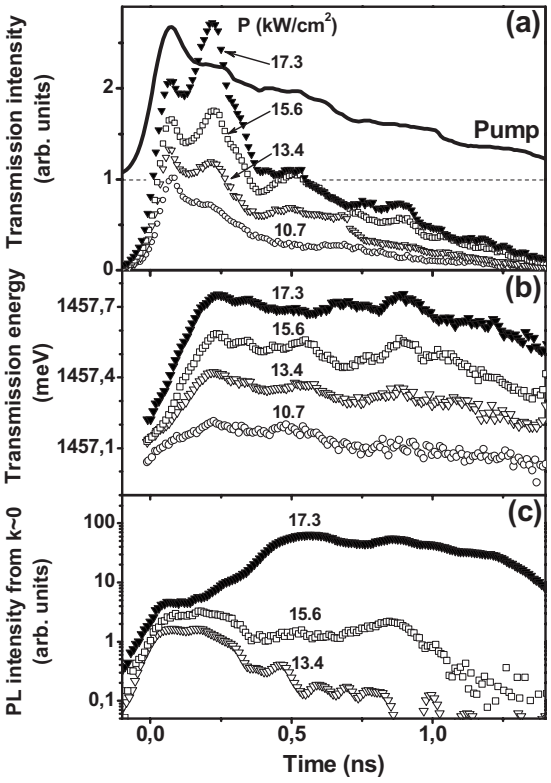

FIG. 2. Time dependences of (a) MC transmission intensity, (b) spectral position of the transmitted signal, and (c) the emission intensity at $k=0$ recorded for several excitation densities below and above the threshold of the stimulated parametric LP-LP scattering $P_{\mathrm{thr}} \sim 15$ kW/cm^2. Pump profile is shown in (a) by a solid line labeled as "Pump."

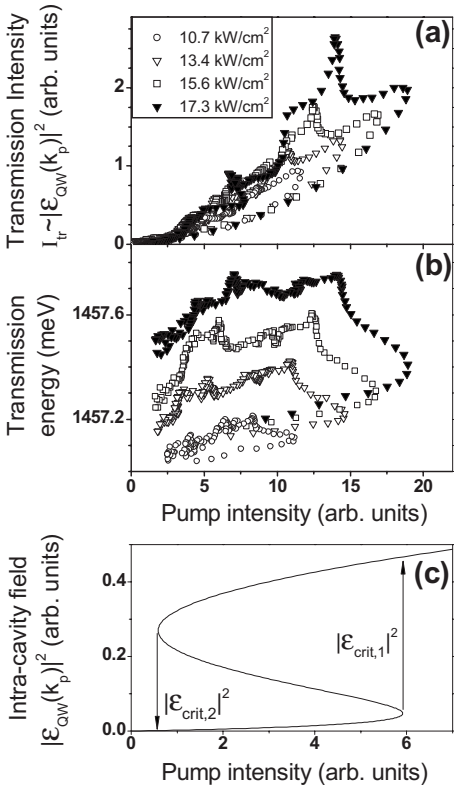

FIG. 3. Measured dependences of (a) intensity and (b) spectral position of the MC transmission signal as a function of the external field intensity for excitation densities below, close to, and above the threshold for the stimulated parametric LP-LP scattering $P_{\mathrm{thr}} \sim 15$ kW/cm^2. Panel (c) shows a typical single-mode response of the intracavity field to the external pump, calculated for a nonlinear exciton oscillator.

and a strong blueshift of the signal. Former behavior is characteristic for the driven mode in the nearly linear regime, while the latter one is the fingerprint of the highly nonlinear regime.

First, we consider the dynamics of the intracavity electric field. Time evolutions of the MC transmission intensity $I_{\mathrm{tr}}(t)$ are presented in Fig. 2(a) for several excitation densities P in the range from 10.7 to 17.3 kW/cm^2. $I_{\mathrm{ext}}(t)$ is also shown, labeled as "Pump." At the lowest $P=10.7$ kW/cm^2, $I_{\mathrm{tr}}(t)$ [and, hence, $|\mathcal{E}_{\mathrm{QW}}(\mathbf{k}_p,t)|^2$] increases slightly superlinearly with $I_{\mathrm{ext}}(t)$, reaches the maximum, and then decreases slightly superlinearly with $I_{\mathrm{ext}}(t)$. Such a behavior is a characteristic of a weakly excited nonlinear oscillator. With increasing P to 13.4 kW/cm^2, the transmission signal starts to show a nonmonotonic dependence on $I_{\mathrm{ext}}(t)$: a short-term peak appears in $I_{\mathrm{tr}}(t)$ on the descending side of the pulse, in the time interval 0.15–0.3 ns. The peak grows quickly with increasing P. The sharp increase in $|\mathcal{E}_{\mathrm{QW}}(\mathbf{k}_p,t)|$ on the backdrop excitation density is the sign of an instability in the pumped LP mode.

In a presentation of $\mathcal{E}_{\mathrm{QW}}$ as a function of $\mathcal{E}_{\mathrm{ext}}$, the hysteresis behavior becomes pronounced. Experimental relationship between $I_{\mathrm{tr}}(t)$ and $I_{\mathrm{ext}}(t)$ redrawn in the form of $I_{\mathrm{tr}}(I_{\mathrm{ext}})$ (equivalent to the dependence $|\mathcal{E}_{\mathrm{QW}}|^2$ as a function of $|\mathcal{E}_{\mathrm{ext}}|^2$) is presented in Fig. 3(a). Figure 3(a) shows that already at $P=10.7$ kW/cm^2, I_{tr} as a function of I_{ext} demonstrates a weak hysteresis. The hysteresis magnitude grows quickly with increasing P, which is indicative of a critical transformation of the driven LP mode, related to its bistability.

Bistability of the driven LP mode is typical of a nonlinear classical oscillator.[41] For a resonantly driven exciton condensate it was formerly predicted in Ref. 35. At last, in the LP system it was actually observed in Ref. 24 for the case of pump directed by the cavity normal. But although theoretical explanation of the bistability presumes the same effect irrespective of pump direction, in the case of the pump imposed at the magic angle it is not observed in the form of a typical hysteresis under the action of cw excitation. A reason for that is the presence of another type of instability in the driven system—parametric decay of the driven mode, which makes the situation more complicated.[36,38] To make the difference evident, we compare results of our experiment with an exact single-mode approximation.

A typical relationship between $|\mathcal{E}_{\mathrm{QW}}|$ and $|\mathcal{E}_{\mathrm{ext}}|$ for a nonlinear excitonic oscillator predicted in a single-mode approximation (i.e., if only the driven mode is taken into account) is shown in Fig. 3(c). There are two stable branches, an upper and a lower one, with $d|\mathcal{E}_{\mathrm{QW}}|^2/d|\mathcal{E}_{\mathrm{ext}}|^2>0$.[41,42] The lower stable branch $|\mathcal{E}_{\mathrm{QW}}|(|\mathcal{E}_{\mathrm{ext}}|)$ is superlinear and reversible below a critical value $|\mathcal{E}_{\mathrm{ext}}^{(\mathrm{crit},1)}|$. An abrupt transition into the upper stable branch occurs when $|\mathcal{E}_{\mathrm{ext}}|$ reaches the critical value. A reverse transition to the lower stable branch for the

decreasing field takes place at $|\mathcal{E}_{\text{ext}}|=|\mathcal{E}_{\text{ext}}^{(\text{crit},2)}|<|\mathcal{E}_{\text{ext}}^{(\text{crit},1)}|$, resulting in a hysteresis behavior of $|\mathcal{E}_{\text{QW}}|(|\mathcal{E}_{\text{ext}}|)$.

Comparison of measured and calculated relationships between $|\mathcal{E}_{\text{QW}}|^2$ and $|\mathcal{E}_{\text{ext}}|^2$ in Figs. 3(a) and 3(c) reveals two significant discrepancies. First, the steplike increase in $|\mathcal{E}_{\text{QW}}|$ occurs not on the increasing but on the decreasing side of the pulse, which cannot be explained in the single-mode approximation. Second, the experiment shows that the increase in $|\mathcal{E}_{\text{QW}}|$ is immediately followed by a steplike decrease (amount of the decrease is dependent on P). Such a behavior suggests that the steplike increase in $|\mathcal{E}_{\text{QW}}(\mathbf{k}_p)|$ brings the LP system into an unstable state, while in the single-mode approximation, this state should be stable until the critical value $|\mathcal{E}_{\text{ext}}^{(\text{crit},2)}|$ is achieved. Moreover, the value of $|\mathcal{E}_{\text{ext}}^{(\text{crit},2)}|$ does not depend on the peak magnitude of $|\mathcal{E}_{\text{ext}}|$ when the latter exceeds $|\mathcal{E}_{\text{ext}}^{(\text{crit},1)}|$. Before consideration of various theoretical models offered to describe the dynamics of $|\mathcal{E}_{\text{QW}}(\mathbf{k}_p)|$, we examine the blueshift for the driven LP mode within the duration of the pulse, which is connected to a repulsive exciton-exciton interaction in the system of circularly polarized LPs.

B. Hysteresis in the blueshift for the driven LP mode

The blueshift of the LP energy is related to the repulsive exciton-exciton interaction and increases with the density of photoexcited excitons.[43] In turn, the blueshift of the driven mode strongly affects the relationship between $\mathcal{E}_{\text{QW}}$ and $\mathcal{E}_{\text{ext}}$ because of the change in the detuning between the energies of the driven LP mode and of the exciting laser, $D_p=\hbar\omega_p-\tilde{E}_{\text{LP}}(\mathbf{k}_p)$. The FWHM of the exciting pump used in our studies slightly exceeds that of the LP mode resonance. As a result, the spectral distribution of the intracavity field is slightly shifted from $\tilde{E}_{\text{LP}}(\mathbf{k}_p)$ to the pump pulse maximum. However in view of a monotonous correlation between the blueshifts in $E_{\text{tr}}(t)$ and $\tilde{E}_{\text{LP}}(\mathbf{k}_p)$, the time profile of $E_{\text{tr}}(t)$ reflects the behavior of the resonance energy $\tilde{E}_{\text{LP}}(\mathbf{k}_p)$.

Changes in the spectral distribution of the intracavity field at the excitation wave vector during the excitation pulse are shown in Fig. 1(a). Excitation at $P=11.3$ kW/cm^2, i.e., below the threshold density, causes a very weak blueshift in the transmission peak (not exceeding 0.1 meV) and a small change in the line FWHM. At $P=17.3$ kW/cm^2, the spectra demonstrate a strong (exceeding 50%) increase in the line FWHM and a strong blueshift of the transmission signal which exceeds 0.5 meV for t between 0.3 and 1 ns. As a result, the transmission signal shifts slightly above the exciting pulse.

Time dependence of spectral position of the transmission signal, $E_{\text{tr}}(t)$, is shown in Fig. 2(b) for several excitation intensities. Comparison of time profiles for the excitation pulse $|\mathcal{E}_{\text{ext}}(t)|^2$ and for the electric field $|\mathcal{E}_{\text{QW}}(\mathbf{k}_p,t)|^2$ displayed in Fig. 2(a) with that for the blueshift in E_{tr} in Fig. 2(b) shows that they strongly differ from each other. The blueshift of $E_{\text{tr}}(t)$ follows neither $|\mathcal{E}_{\text{ext}}(t)|^2$ nor $|\mathcal{E}_{\text{QW}}(\mathbf{k}_p,t)|^2$.

Figure 3(b) demonstrates that the blueshift in E_{tr} plotted as a function of I_{ext} also demonstrates the hysteresis behavior. The hysteresis appears at a relatively low excitation density and increases with P. The difference in E_{tr} at the two sides of the hysteresis curve is less than 0.1 meV at $P=10.7$ kW/cm^2 and increases to ~0.6 meV at $P=17.3$ kW/cm^2.

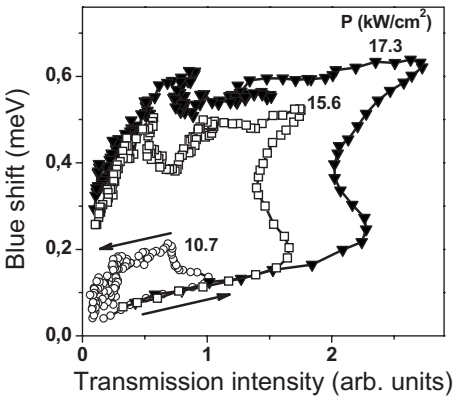

FIG. 4. Measured dependence of the blueshift in spectral position of the transmission signal as a function of the signal intensity for excitation densities below, close to, and above the threshold for the stimulated parametric LP-LP scattering ($P_{\text{thr}}\approx 15$ kW/cm^2).

In Fig. 4, the blueshift ΔE_{tr} is presented as a function of I_{tr}. One can see that a linear relationship between ΔE_{tr} and $|\mathcal{E}_{\text{QW}}(\mathbf{k}_p)|^2$, which is characteristic of the case of predominant occupation of the driven LP mode, is observed only in the beginning of the pulse. The blueshift of E_{tr} does not stop its growth when $|\mathcal{E}_{\text{QW}}(\mathbf{k_p})|^2$ reaches its first maximum; on the contrary, it continues growing while $|\mathcal{E}_{\text{QW}}(\mathbf{k_p})|^2$ decreases. Such an effect can be observed only due to the occupation of the states other than $\mathbf{k}=\mathbf{k}_p$. On the other hand, Fig. 2(c) shows that the decrease in $|\mathcal{E}_{\text{QW}}(\mathbf{k_p})|^2$ in the time range of t ~0.2–0.3 ns is not followed by any strong increase in occupation of the signal states at $k=0$. Indeed, the occupation of the $k=0$ mode remains weak at $P=15.6$ kW/cm^2 over the whole duration of the pulse, while at $P=17.3$ kW/cm^2 strong increase in its occupation starts with a delay of more than 100 ps after the sharp decrease in $\mathcal{E}_{\text{QW}}(\mathbf{k_p})$. The idler at $\mathbf{k}=2\mathbf{k_p}$ (not displayed in Fig. 2) shows a similar behavior. Thus, we can conclude that the LPs that maintain the permanence of the blueshift in the driven LP mode during a sharp decrease in $\mathcal{E}_{\text{QW}}(\mathbf{k}_p)$ are distributed over a large range of wave vectors rather than being concentrated in the signal and idler modes. This conclusion is a direct confirmation that the three-mode (pump, signal, and idler) OPO model[22,29] is not sufficient for the explanation of the experimentally observed hysteresis in the dependences of $E_{\text{tr}}(|\mathcal{E}_{\text{ext}}|)$.

Finally, we examine the behavior of the resonance energy of the driven LP mode for the upper branch of the hysteresis loop $\Delta E_{\text{tr}}(I_{\text{ext}})$. In this case the excited polariton system has already passed through the threshold for the parametric instability with respect to the LP-LP scattering. Figure 3(b) shows that ΔE_{tr} remains nearly constant over a wide range of the pumping density. The blueshift starts to decrease only when the exciting density falls down nearly twice. Such a stabilization of the resonance energy of the driven LP mode in this range is maintained due to the energy shift of the mode above the energy of the exciting laser. The latter can be clearly seen in Fig. 1(b). Such a shift provides a negative

feedback in the pumped LP system, which stabilizes both the LP density and the blueshift in the driven LP mode. Indeed, a decrease in the excited polariton density causes a decrease in $\tilde{E}_{\mathrm{LP}}(\mathbf{k}_p)$, which moves the driven mode closer to the resonance with the exciting laser. This causes an increase in the inner MC field, which, in turn, leads to the growth in the excited LP density, preventing a decrease in the blueshift. In that way, both the high density of scattered LPs and, along with it, the blueshift in the driven mode remain nearly constant over a rather wide range of decreasing excitation density.

The discussed reason for the stabilization of E_{tr} is similar to that for a bistable nonlinear oscillator, which is shown in Fig. 3(c). However the stabilization is maintained in that case by a high population of the driven mode itself. On the contrary, Fig. 4 shows that E_{tr} remains nearly constant in our case over a threefold decrease in $|\mathcal{E}_{\mathrm{QW}}(\mathbf{k}_p)|^2$. Hence, the stability of the energy of the driven mode is supported by LPs scattered from this mode in process of the highly efficient stimulated LP-LP scattering.

C. Instabilities and hysteresis behavior of the driven LP mode: Effect of coherent scattering of LPs

Going beyond the framework of a few-mode approximation, which does not explain the observed instabilities in the driven LP mode, one should take into account all the pairwise interactions in the many-body system of the MC polaritons. The most advanced available model is based on a system of coupled equations for the exciton polarization $\mathcal{P}(\mathbf{k},t)$ and the intracavity electric field $\mathcal{E}_{\mathrm{QW}}(\mathbf{k},t)$ that take the external pumping into account:[30,31]

$$\left[i\hbar\frac{d}{dt} - E_C(\mathbf{k})\right]\mathcal{E}_{\mathrm{QW}}(\mathbf{k},t) = \alpha(\mathbf{k})\mathcal{E}_{\mathrm{ext}}(\mathbf{k},t) + \beta(\mathbf{k})\mathcal{P}(\mathbf{k},t), \tag{1}$$

$$\left[i\hbar\frac{d}{dt} - E_X\right]\mathcal{P}(\mathbf{k},t) = A\mathcal{E}_{\mathrm{QW}}(\mathbf{k},t) + V\sum_{\mathbf{q}_1,\mathbf{q}_2}\mathcal{P}^*(\mathbf{q}_1+\mathbf{q}_2 - \mathbf{k},t)\mathcal{P}(\mathbf{q}_1,t)\mathcal{P}(\mathbf{q}_2,t) + \xi(\mathbf{k},t). \tag{2}$$

Here, $\mathcal{E}_{\mathrm{ext}}(\mathbf{k},t)=\delta_{\mathbf{k},\mathbf{k}_p}\mathcal{E}(t)\exp(-iE_pt/\hbar)$ is the excitation field, $E_C(\mathbf{k})$ and E_X are the cavity photon and exciton energies, respectively, V is the exciton-exciton interaction constant, A is the exciton polarizability, and $\xi(\mathbf{k},t)$ is a stochastic Langevin force [$\langle\xi(\mathbf{k},t)\rangle=0$ and $\langle\xi(\mathbf{k},t)\xi(\mathbf{k}',t')\rangle\propto\delta_{\mathbf{k},\mathbf{k}'}\delta_{t,t'}$]. Cavity response coefficients $\alpha(\mathbf{k})$ and $\beta(\mathbf{k})$ are calculated using the transfer-matrix technique.

This approximation, which allows one to take into account all of the pairwise interactions in a coherent many-mode polariton system, will be referred to as a coherent many-mode approximation. The equation for exciton polarization is similar to the Gross-Pitaevskii equation.[44] This approximation was recently found to describe qualitatively the stimulated polariton scattering under a strong resonant excitation.[34,36,38,45]

Figure 5 shows calculated time dependences of $|\mathcal{E}_{\mathrm{QW}}(\mathbf{k}_p,t)|^2$ and $\tilde{E}_{\mathrm{LP}}(\mathbf{k}_p,t)$ for two excitation densities slightly above the threshold. The cavity parameters and the excitation pulse shape approximately correspond to the experimental conditions.[46] Effective resonance energy $\tilde{E}_{\mathrm{LP}}$ of the driven mode depending on the exciton polarization $\mathcal{P}$ (in all k-space modes) is calculated in agreement with quasistationary representation of the response function:

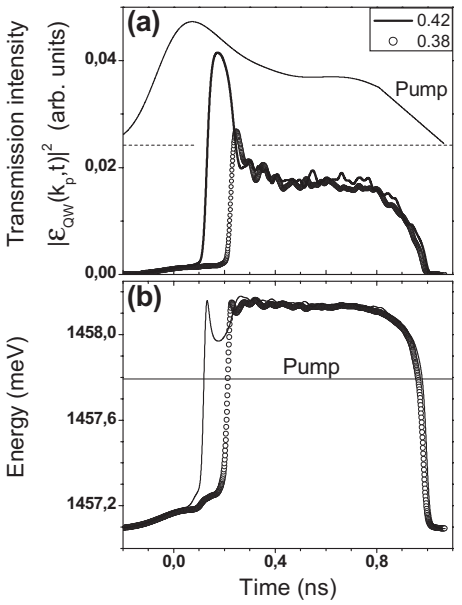

FIG. 5. Time dependences of (a) internal MC electric field and (b) driven LP mode energy (relative to QW exciton energy E_X) calculated in the coherent many-mode approximation for the pump profile displayed in (a) by solid line at two excitation intensities: close to the threshold (P=0.38) and 10% above it (P=0.42).

$$|\mathcal{P}(\mathbf{k}_p)|^2 \propto \frac{|\mathcal{E}_{\mathrm{ext}}|^2}{[E_p - \tilde{E}_{\mathrm{LP}}(\{\mathcal{P}\})]^2 + [\hbar\tilde{\gamma}_{\mathrm{LP}}(\{\mathcal{P}\})]^2}, \tag{3}$$

where $\tilde{\gamma}_{\mathrm{LP}}$ is the corresponding decay coefficient.

The deviation from the single-mode approximation starts at relatively high excitation densities because of the small LP-LP scattering rate at low LP densities. The path of the instability development and the hysteresis shapes for either $|\mathcal{E}_{\mathrm{QW}}(\mathbf{k}_p)|$ or E_{tr} as a function of $|\mathcal{E}_{\mathrm{ext}}|$ depend on the time profile of the excitation. Such a behavior is caused by the feedback effect of the scattered LPs on the state of the driven mode.

Comparison of the simulation results displayed in Fig. 5(a) with the experimental data in Fig. 2(a) demonstrates that the simulations reproduce qualitatively both the steplike increase in $|\mathcal{E}_{\mathrm{QW}}|$ and its subsequent rapid decrease. Calculations show that the increase is caused by the self-instability of the driven LP mode. However, the upper state for this transition turns out to be unstable due to development of parametric LP-LP scattering. The instability of the driven LP mode with respect to the intermode scattering results in a rapid occupation of LP states in a wide range of wave vectors (rather than the only two—signal and idler—modes taken into account in the three-mode OPO model). Comparison of calculated dependences $|\mathcal{E}_{\mathrm{QW}}(\mathbf{k}_p,t)|^2$ and $\tilde{E}_{\mathrm{LP}}(\mathbf{k}_p,t)$ in Fig. 5

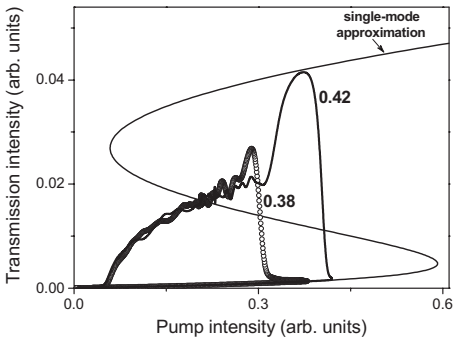

FIG. 6. Dependences of MC transmission signal as a function of the pump intensity calculated in the coherent many-mode approximation. Both for the pump profile shown in Fig. 5, the two excitation intensities $P=0.38$ and $P=0.42$ (same as in Fig. 5) are used. The signal calculated in the single-mode approximation ("S"-shaped curve) is also shown for comparison.

shows that the coherent many-mode OPO model reproduces the absence of a noticeable decrease in $\tilde{E}_{\mathrm{LP}}(\mathbf{k}_p)$ when $|\mathcal{E}_{\mathrm{QW}}(\mathbf{k}_p)|$ decreases strongly due to the parametric instability, in good agreement with the experimental data in Fig. 2. Calculations show that the stability of $\tilde{E}_{\mathrm{LP}}(\mathbf{k}_p)$ is maintained by a contribution from the scattered LPs to the blueshift in the driven mode. An unusually low threshold and a high efficiency of the parametric scattering of the driven LP mode, which supports a fast growth of the overall LP density in the MC, are related to presence of the inflection point in the LP dispersion curve, due to which both the energy and the momentum conservation laws are simultaneously fulfilled.

In Fig. 6, the developments of the driven mode instability are compared for single-mode and many-mode coherent approximations. One can see that the latter approximation predicts a much lower threshold. A decrease in the critical field $|\mathcal{E}_{\mathrm{ext}}^{(\mathrm{crit},1)}|$ is related to the positive feedback of the scattered LPs on the blueshift in the driven mode, in the case when the intermode decay instability develops before the self-instability in the driven mode.[47] In that case, the LP-LP scattering leads to an increase in the overall LP density, the contribution of which to the blueshift in the resonance energy results in an effective decrease in the detuning $D_p=E_p-\tilde{E}_{\mathrm{LP}}(\mathbf{k}_p)$. As a result the unique dependence of E_{LP} and, hence, of $\mathcal{E}_{\mathrm{QW}}$ on $\mathcal{E}_{\mathrm{ext}}$ at the excitation wave vector is disturbed. That allows the transition point to shift to the decreasing side of the excitation pulse, in agreement with the experiment. The results of numerical simulations displayed in Fig. 6 show that for the pulse shape similar to that used in the experiment, the shift can be as large as 30%.

Thus, the coherent many-mode approximation provides a qualitative description of the main features of the instabilities and the hystereses in a resonantly pumped LP system, both for the magnitude of the internal optical field and for the blueshift in the LP resonance. More detailed comparison of the modeling with the experiment reveals significant quantitative and even qualitative discrepancies. In particular, according to numerical modeling, the reverse transition of the driven mode to the lower state should be followed by an abrupt decrease in its energy, with a characteristic time of about 20 ps, which corresponds to the lifetime of LPs with $k\sim(3-5)k_{\mathbf{p}}$. Meanwhile, in the experimental data in Fig. 2, the decrease time is about an order of magnitude larger, in the range of 200–300 ps. Such long times are typical for excitonlike states with large wave vectors. Such states can be efficiently generated, in particular, due to an incoherent scattering of the pumped LPs by phonons and/or free electrons,[16,48–50] which is not taken into account in the suggested coherent model.

IV. CONCLUSION

Dynamics of the driven LP mode has been investigated in a GaAs MC under a nanosecond-long resonant pumping incident at the magic angle slightly above the dispersion curve. Time-resolved measurements have revealed an interplay between two parametric instabilities in the LP system, both related to the LP-LP interaction. These are, first, instability of the driven mode by itself (which is connected to the single-mode bistability) and, second, the instability with respect to the intermode LP-LP scattering.

In the present study, the initial process of the instability development has been traced in detail, by means of the time-resolved measurement of both energy and intensity distributions of the transmission signal. We have found that the critical excitation density for the transition connected to the single-mode bistability of the driven LP mode is lowered due to additional mode blueshift induced by LPs scattered into a wide range of wave vectors. The steplike increase in $|\mathcal{E}_{\mathrm{QW}}(\mathbf{k}_p)|$ caused by this transition transfers the LP system into the state of strong parametric instability. As a result, the final state for the transition is unstable, with respect to the intermode scattering causing a sharp decrease in $|\mathcal{E}_{\mathrm{QW}}(\mathbf{k}_p)|$. The magnitude of the decrease is determined by the energy balance of the open dissipative system of numerous LP modes interacting with each other. Such a behavior is qualitatively different from that of excitons in semiconductors and, in general, occurs due to the presence of the inflection point in the microcavity polariton dispersion curve.

The discovered dynamics of the driven LP mode cannot be described even qualitatively in the framework of single- and three-mode OPO models. A qualitative explanation of the observed instabilities and the hysteresis behavior of the driven LP mode has been achieved in the framework of a coherent multimode approximation. One of possible reasons for remaining quantitative disagreement could be the effect of the incoherent scattering of driven polaritons by phonons and free carriers, which is neglected in the suggested theoretical model. Such a scattering, which transforms the short-lifetime (3–5 ps) LPs into long-lifetime excitonlike states, leads to an effective increase in the average exciton density and, as a consequence, leads to an additional blueshift in the driven LP mode and affects the development of the instabilities in the pumped LP system.

ACKNOWLEDGMENTS

We thank N. A. Gippius and S. G. Tikhodeev for fruitful discussions, I. E. Itskevitch for critical reading of paper and valuable remarks, M. S. Skolnick for rendered samples, and M. N. Makhonin for help in the experiment and discussions. This work was supported by the Russian Foundation for Basic Research and the Russian Academy of Sciences.

[1] C. Weisbuch, M. Nishioka, A. Ishikawa, and Y. Arakawa, Phys. Rev. Lett. **69**, 3314 (1992).
[2] M. S. Skolnick, T. A. Fisher, and D. M. Whittaker, Semicond. Sci. Technol. **13**, 645 (1998).
[3] G. Khitrova, H. M. Gibbs, F. Jahnke, M. Kira, and S. W. Koch, Rev. Mod. Phys. **71**, 1591 (1999).
[4] R. Houdré, J. L. Gibernon, P. Pellandini, R. P. Stanley, U. Oesterle, C. Weisbuch, J. O'Gorman, B. Roycroft, and M. Ilegems, Phys. Rev. B **52**, 7810 (1995).
[5] L. S. Dang, D. Heger, R. Andre, F. Boeuf, and R. Romestain, Phys. Rev. Lett. **81**, 3920 (1998).
[6] P. Senellart and J. Bloch, Phys. Rev. Lett. **82**, 1233 (1999).
[7] A. Imamoglu, R. J. Ram, S. Pau, and Y. Yamamoto, Phys. Rev. A **53**, 4250 (1996).
[8] M. Muller, J. Bleuse, R. Andre, and H. Ulmer-Tuffigo, Physica B **272**, 476 (1999).
[9] A. I. Tartakovskii, V. D. Kulakovskii, D. N. Krizhanovskii, M. S. Skolnick, V. N. Astratov, A. Armitage, and J. S. Roberts, Phys. Rev. B **60**, R11293 (1999).
[10] R. Huang, F. Tassone, and Y. Yamamoto, Phys. Rev. B **61**, R7854 (2000).
[11] R. M. Stevenson, V. N. Astratov, M. S. Skolnick, D. M. Whittaker, M. Emam-Ismail, A. I. Tartakovskii, P. G. Savvidis, J. J. Baumberg, and J. S. Roberts, Phys. Rev. Lett. **85**, 3680 (2000).
[12] J. J. Baumberg, P. G. Savvidis, R. M. Stevenson, A. I. Tartakovskii, M. S. Skolnick, D. M. Whittaker, and J. S. Roberts, Phys. Rev. B **62**, R16247 (2000).
[13] P. G. Savvidis, J. J. Baumberg, R. M. Stevenson, M. S. Skolnick, D. M. Whittaker, and J. S. Roberts, Phys. Rev. Lett. **84**, 1547 (2000).
[14] A. I. Tartakovskii, D. N. Krizhanovskii, and V. D. Kulakovskii, Phys. Rev. B **62**, R13298 (2000).
[15] D. N. Krizhanovskii, A. I. Tartakovskii, A. V. Chernenko, V. D. Kulakovskii, M. Emam-Ismail, M. S. Skolnick, and J. S. Roberts, Solid State Commun. **118**, 583 (2001).
[16] G. Malpuech, A. Kavokin, A. Di Carlo, and J. J. Baumberg, Phys. Rev. B **65**, 153310 (2002).
[17] A. I. Tartakovskii, D. N. Krizhanovskii, G. Malpuech, M. Emam-Ismail, A. V. Chernenko, A. V. Kavokin, V. D. Kulakovskii, M. S. Skolnick, and J. S. Roberts, Phys. Rev. B **67**, 165302 (2003).
[18] C. Ciuti, P. Schwendimann, B. Deveaud, and A. Quattropani, Phys. Rev. B **62**, R4825 (2000).
[19] P. G. Savvidis, C. Ciuti, J. J. Baumberg, D. M. Whittaker, M. S. Skolnick, and J. S. Roberts, Phys. Rev. B **64**, 075311 (2001).
[20] V. D. Kulakovskii, A. I. Tartakovskii, D. N. Krizhanovskii, N. A. Gippius, M. S. Skolnick, and J. S. Roberts, Nanotechnology **12**, 475 (2001).
[21] R. Butté, M. S. Skolnick, D. M. Whittaker, D. Bajoni, and J. S. Roberts, Phys. Rev. B **68**, 115325 (2003).
[22] C. Ciuti, P. Schwendimann, and A. Quattropani, Phys. Rev. B **63**, 041303(R) (2001).
[23] D. M. Whittaker, Phys. Rev. B **63**, 193305 (2001).
[24] A. Baas, J. Ph. Karr, H. Eleuch, and E. Giacobino, Phys. Rev. A **69**, 023809 (2004).
[25] A. Baas, J. Ph. Karr, M. Romanelli, A. Bramati, and E. Giacobino, Phys. Rev. B **70**, 161307(R) (2004).
[26] D. M. Whittaker, Phys. Rev. B **71**, 115301 (2005).
[27] I. Carusotto and C. Ciuti, Phys. Rev. Lett. **93**, 166401 (2004).
[28] D. M. Whittaker, Phys. Status Solidi C **2**, 733 (2005).
[29] M. Wouters and I. Carusotto, Phys. Rev. B **75**, 075332 (2007).
[30] N. A. Gippius, S. G. Tikhodeev, V. D. Kulakovskii, D. N. Krizhanovskii, and A. I. Tartakovskii, Europhys. Lett. **67**, 997 (2004).
[31] N. A. Gippius and S. G. Tikhodeev, J. Phys.: Condens. Matter **16**, S3653 (2004).
[32] S. S. Gavrilov, N. A. Gippius, V. D. Kulakovskii, and S. G. Tikhodeev, JETP **104**, 715 (2007).
[33] N. A. Gippius, S. G. Tikhodeev, L. V. Keldysh, and V. D. Kulakovskii, Phys. Usp. **48**, 306 (2005).
[34] V. D. Kulakovskii, D. N. Krizhanovskii, M. N. Makhonin, A. A. Demenev, N. A. Gippius, and S. G. Tikhodeev, Phys. Usp. **48**, 312 (2005).
[35] V. F. Elesin and Yu. V. Kopayev, Zh. Eksp. Teor. Fiz. **63**, 1447 (1972) [Sov. Phys. JETP **36**, 767 (1973)].
[36] D. N. Krizhanovskii, S. S. Gavrilov, A. P. D. Love, D. Sanvitto, N. A. Gippius, S. G. Tikhodeev, V. D. Kulakovskii, D. M. Whittaker, M. S. Skolnick, and J. S. Roberts, Phys. Rev. B **77**, 115336 (2008).
[37] C. Richy, K. I. Petsas, E. Giacobino, C. Fabre, and L. Lugiato, J. Opt. Soc. Am. B **12**, 456 (1995).
[38] A. A. Demenev, A. A. Shchekin, A. V. Larionov, S. S. Gavrilov, V. D. Kulakovskii, N. A. Gippius, and S. G. Tikhodeev, Phys. Rev. Lett. **101**, 136401 (2008).
[39] We introduce the term "quasistationary excitation" first of all in order to distinguish our excitation regime from the picosecond-long pulse excitation employed in a large number of preceding experiments [e.g., W. Langbein, Phys. Rev. B **70**, 205301 (2004)]. In the experiments with pulse duration comparable with polariton lifetime (of one to few picoseconds), neither the stimulated scattering into $k=0$ (without a probe laser) nor the bistability effect is observed. "Stationarity" of a dynamical regime is considered in comparison with the longest characteristic times of the system. First, our excitation regime obeys the condition of a very smooth variation in pump within the lifetime of polariton. At the same time, characteristic times markedly exceeding the lifetime of polariton appear due to collective effects in the many-mode system. Our experiment shows that they reach few hundreds of picoseconds, which is still smaller than the pump pulse duration of 1 ns. Note as well that the pattern of stimulated scattering in the time range close to the end of the pulse reaches the state very similar to that in the cw experiments (Ref. 38).

Thus, although the excitation conditions in our study cannot be considered as exactly stationary, they are close to them. The scope of our consideration is close to that of Refs. 22–27 just because we can still use the coherent mean-field approximation and, consequently, the concepts of energy renormalization, parametric scattering, etc.

[40] A mixed representation of $\mathcal{E}_{QW}$ as a function of both time and frequency corresponds to experimental conditions when each point on the time scale is averaged over ~ 70 ps.

[41] G. Duffing, *Erzwungene Schwingungen bei Veränderlicher Eigenfrequenz* (Vieweg, Braunschweig, Germany, 1918).

[42] H. M. Gibbs, *Optical Bistability: Controlling Light with Light* (Academic, New York, 1985).

[43] N. Peyghambarian, H. M. Gibbs, J. L. Jewell, A. Antonetti, A. Migus, D. Hulin, and A. Mysyrowicz, Phys. Rev. Lett. **53**, 2433 (1984).

[44] L. P. Pitayevskii and S. Stingari, *Bose-Einstein Condensation* (Clarendon, Oxford, 2003).

[45] M. N. Makhonin, A. A. Demenev, S. S. Gavrilov, V. D. Kulakovskii, N. A. Gippius, and S. G. Tikhodeev, Solid State Commun. **144**, 384 (2007).

[46] Parameters used in the calculation are the following: MC quality factor is 4.2×10^3; lifetimes of a "free" exciton and a cavity photon at $\mathbf{k}=0$ are 16.5 and 3.8 ps, respectively; effective mass of cavity photon at $\mathbf{k}=0$ is $\sim 3 \times 10^{-32}$ g (MC spectrum is calculated using the transfer-matrix technique); Rabi splitting is 6.4 meV; pump wave number is 1.8 μm^{-1}; and pump detuning from the LP mode is 0.7 meV. Equations (1) and (2) are solved on the rectangular mesh in momentum space with the step of 0.15 μm^{-1} in both k_x and k_y directions (k_x and k_y vary from -4.2 to 7.8 μm^{-1} and from -3.0 to 3.0 μm^{-1}, respectively).

[47] S. S. Gavrilov (unpublished).

[48] D. N. Krizhanovskii, A. I. Tartakovskii, M. N. Makhonin, A. N. Dremin, and V. D. Kulakovskii, Phys. Rev. B **70**, 195303 (2004).

[49] P. G. Lagoudakis, M. D. Martin, J. J. Baumberg, A. Qarry, E. Cohen, and L. N. Pfeiffer, Phys. Rev. Lett. **90**, 206401 (2003).

[50] M. Perrin, P. Senellart, A. Lemaître, and J. Bloch, Phys. Rev. B **72**, 075340 (2005).